Analytical Modeling of Thermal Stress Relieving in Stainless and High Strength Steel Weldments

One-dimensional analysis is extended for calculating residual stresses after the welding of thin plates and subsequent stress relief heat treatment

BY J. E. AGAPAKIS AND K. MASUBUCHI

ABSTRACT. An analytical and experimental investigation of the effectiveness of stress relief heat treatments — in terms of the attained reduction of residual stresses — is presented. A cost-effective analytical model is employed for the calculation of temperatures, strains and stresses during and after welding and subsequent stress relief heat treatments of thin plates. Stress relaxation due to creep at high temperatures is modeled. Any temperature history during the heat treatment can be input to the model. Uniform temperature heating in a furnace and line heating with a flame are further examined.

Initial verification experiments are performed with ⅜ in. (9.5 mm) thick Type 304 stainless steel plates. The specimens are edge-welded and stress relieved in a furnace. The plates are finally sectioned, and residual stresses are measured by stress relaxation. Some further experiments are also performed with ½ in. (12.7 mm) thick HY-130 high strength steel plates. Good correlation between experimental results and analytical predictions can be obtained, if the model assumptions are not seriously violated.

Paper presented at the 64th Annual AWS Convention held in Philadelphia, Pennsylvania, during April 25-29, 1983.

J. E. AGAPAKIS is a Research Assistant and K. MASUBUCHI is Professor of Ocean Engineering and Materials Science, Massachusetts Institute of Technology, Cambridge, Massachusetts.

Introduction

During welding, local nonuniform heating and subsequent cooling cause the development of complex thermal strains and stresses that finally lead to residual stresses and distortion. These effects are usually detrimental — directly or indirectly — to the integrity and the service behavior of a welded structure. In particular, high tensile residual stresses in the region near the weld might promote brittle fracture, change the fatigue strength, or lead — under suitable environmental conditions — to stress corrosion cracking. Compressive residual stresses combined with initial distortion may reduce the buckling strength, whereas excessive distortion might directly prevent the structure from performing its intended function (Ref. 1).

Several methods aimed at reducing or redistributing residual stresses have been proposed and are currently in use. These include both postweld mechanical and stress relief heat treatments. The latter basically involve heating of the weldment, or of the structure as a whole, to an elevated temperature, and holding at that temperature in order to permit stress relaxation. This is followed by slow cooling to prevent the reintroduction of stresses. Due to the required high temperatures, stress relief heat treatments typically have undesirable effects on the microstructure and mechanical properties of both the base metal and the weld metal. Although such effects can be avoided when stress relieving by mechanical means (through overstressing or vibratory treatments), mechanical means are usually less effective and not universally accepted.

In order to judge the effectiveness of a stress relief heat treatment with regard to the accomplished reduction of residual stresses, it should be necessary to measure the maximum residual stresses before and after the treatment. The difference would be a realistic measure of performance. However, an acceptable alternative to the time-consuming, costly, and usually destructive residual stress measurements, would be a proper analytical model. Furthermore, such a model would be very helpful in determining — by a series of parametric analyses — an optimal lower temperature heat treatment, where a properly selected heating pattern would most effectively reduce or redistribute stresses while keeping the metallurgical changes minimal.

In the past, various investigators devoted extensive research efforts to the analysis of residual stresses and their consequences. Recently at M.I.T., an over ten-year long research program dealing with this subject has been completed. In the course of this program, analytical and numerical models were developed for the analysis of heat transfer, transient and residual stresses, and fracture characteristics of weldments (Refs. 1, 2).

The study reported in this paper was undertaken in order to integrate the aspects of both analysis and control of

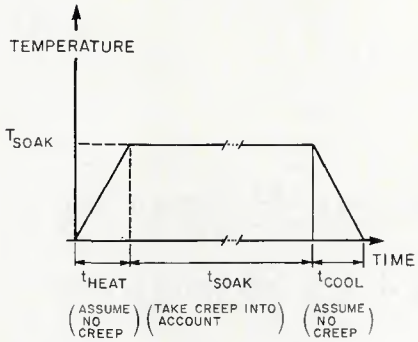

Fig. 1 — Temperature history during stress relief heat treatments

residual stresses associated with welding. The effectiveness of stress relief heat treatments in terms of the attained reduction of residual stresses was both analytically and experimentally investigated (Refs. 2, 3, and 4). Analytical models developed for welding were extended so as to also handle a subsequent stress relief heat treatment. Verification experiments were then performed with stainless (Type 304) and high strength (HY-130) steel plate specimens.

Analysis of Residual Stress Relaxation

Background

Residual stress changes can arise during all three stages of a heat treatment. Referring to Fig. 1, during the heating part of the process, residual stresses decrease due to the temperature dependence of the mechanical properties (mainly through a reduction of the yield strength with temperature). During the holding (or soaking) period, the temperature is kept constant, and residual stresses are reduced due to creep. Finally, during the cool-down period, residual stresses increase due to the temperature dependence of the mechanical properties, but hopefully (when the treatment is successful) not to their initial levels (Ref. 5).

In analyzing the residual stress relaxation during heat treatments, various approaches have been followed by different investigators. Very simple uniform residual stress distributions are usually assumed so that the uniaxial stress-strain curves of the material can be directly employed. Such analytical results are obtained and experimentally tested by Tanaka (Ref. 6).

For more complex cases and two- or three-dimensional stress states, numerical models have been proposed to handle the thermal-elastic-plastic and creep analyses required. Ueda and Fukuda presented a finite element model capable of calculating welding residual stresses and stress relief due to creep (Ref. 7). Fujita *et al.* developed a thermo-visco-elastic-plastic model to study the mechanism of stress relief annealing (Ref. 8). Cameron and Pemberton proposed a numerical model of the thermal stress relief in thin shells of revolution (Ref. 9). Finally, Josefson in a recent study, employed axisymmetric finite element analysis to calculate the redistribution of residual stresses during annealing of thin-walled girth welded pipes (Ref. 10).

For the purposes of the study reported here, it was decided not to use the finite element models previously developed at M.I.T. for the analysis of welding residual stresses. This decision was based on the high computer implementation cost which would make parametric analysis infeasible. Instead, a one-dimensional model was developed similar to the one successfully employed at M.I.T. in the past for the prediction of residual stresses in long, thin butt or edge welded plates (Refs. 1, 11). This model was modified to calculate strains and stresses during and after uniform-temperature treatments and line heating with a flame. Stress relaxation due to creep at high temperatures was also included in the model.

Temperature Distribution

For estimating the non-uniform and changing with time temperature distributions during the welding of butt or edge joints in plates (Fig. 2), the following fundamental assumptions are incorporated in the model:

1. The plate is infinitely large and very thin.
2. The welding arc can be modeled as a line heat source and, therefore, no temperature gradient exists through the thickness of the plate (two-dimensional temperature distribution).
3. The temperature distribution is stationary if viewed from a coordinate system moving with the heat source (quasi-stationary case).

The temperature distribution can then be obtained by modifying the well known Rosenthal solution for a line heat source (Refs. 12, 13), as described in Appendix A.

During heat treatment any arbitrary temperature distribution can be input to the model. In this initial study, however, only uniform temperature treatments and flame heating along a line were analyzed. In the former case, a uniform tempera-

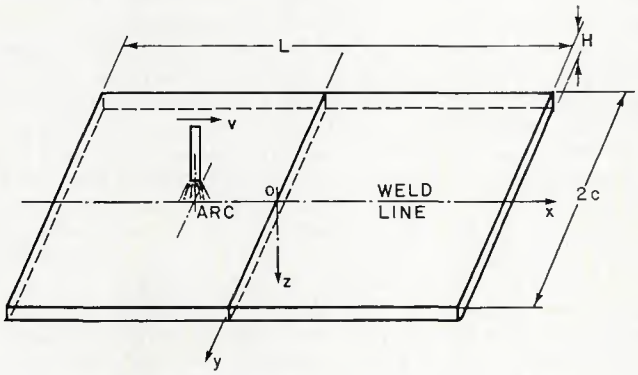

Fig. 2 — Weldment configuration (plates welded using butt joint)

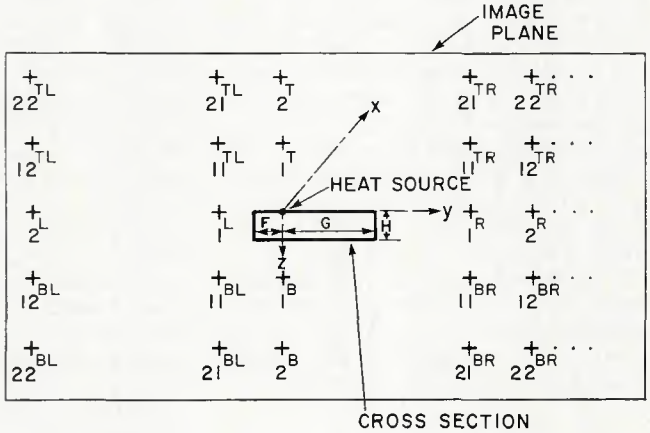

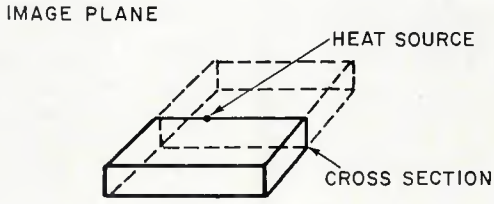

Fig. 3 (right) — Arrangement of the heat source images for a finite-width and finite-thickness plate

ture distribution was assumed over the entire plate, changing with time as in Fig. 1. In the case of line heating, the temperature distribution was calculated in a way analogous to welding, by modifying the Rosenthal solution for a point-heat source moving on a semi-infinite body (Refs. 12, 13). In order to describe the temperature distribution more accurately for the case of a finite width and finite thickness plate heated by a traveling heat source, an infinite series of heat source images have to be used (Fig. 3) as detailed in Appendix A.

Stress Analysis

To calculate the transient and residual stresses during and after welding and subsequent stress relief heat treatments, the method of successive elastic solutions is employed. The procedure, outlined by Mendelson (Refs. 14, 15) was first used in the solution of welding problems by Tall (Ref. 16), and later by Masubuchi *et al.* (Ref. 17).

For the analysis of the stress state at a center cross section of a plate (Fig. 2) due to an arbitrary and changing with time temperature distribution, $\theta(y,t)$, it is assumed that at time t, the section is a part of an infinitely long plate subject to the same temperature distribution over its entire length. This temperature profile is assumed to remain the same during the current time increment, Δt. It is further assumed that stress is non-zero only in the direction of the weld and this stress is only a function of the transverse distance from the weld center line (one-dimensional stress distribution $\sigma_x = \sigma_x(y)$).

If $\sigma_x(y)$ and $\epsilon_x(y)$ are the stress and strain distributions at the end of a time interval Δt, the total strain can then be decomposed to elastic, thermal and inelastic (plastic and creep) components as follows:

$$\epsilon_x(y) = \frac{\sigma_x(y)}{E} + \alpha \cdot (\theta(y) - \theta_o) + \epsilon_x^{in}(y) + \Delta\epsilon_x^{in}(y) \quad (1)$$

where E is the Young's modulus, α the coefficient of thermal expansion, $\epsilon_x^{in}(y)$ the accumulated inelastic strain during the previous time increments, $\Delta\epsilon_x^{in}(y)$ the change of inelastic strain during the current time increment, and θ_o the initial temperature.

Since no external forces and moments act on the plate, the following expression can be derived from global equilibrium for the total strain, $\epsilon_x(y)$, as outlined in Appendix B:

$$\epsilon_x(y) = (A_1 - yA_2) \int_{-c}^{+c} E[\alpha \cdot (\theta(y) - \theta_o) + \epsilon_x^{in}(y) + \Delta\epsilon_x^{in}(y)]dy - (A_2 - yA_3) \int_{-c}^{+c} E[\alpha \cdot (\theta(y) - \theta_o) + \epsilon_x^{in}(y) + \Delta\epsilon_x^{in}(y)]ydy \quad (2)$$

where A_1, A_2, and A_3 can be obtained from the known temperature distribution and the material properties.

The above two equations, together with a uniaxial stress-strain law and a relation between stress and creep strain increments, are sufficient for the solution of the stress problem. Some further required assumptions and the iterative solution procedures are briefly outlined below:

1. During welding and during the heating and cooling stages of a uniform temperature heat treatment (Fig. 1), creep is not taken into account. In that case, the inelastic strain increments are entirely due to plastic deformation. At each time step, it is initially assumed that no plastic strain exists and thus equation (2) can be used for a first approximation of the total and the mechanical strain. From the assumed stress-strain law, a first approximation of the plastic strain can then be obtained. This value can be further used in equation (2) for a second approximation of the total strain, and the process can be repeated until convergence is reached.

2. During the holding stage of heat treatment, it is assumed that residual stresses can be changed only through creep deformation. At each time step, the inelastic strain increments are only due to creep, and the previously accumulated plastic strain remains constant. It is initially assumed that the creep strain increment during each time step is zero, so that a first approximation of the total strain can be obtained from equation (2). This value can be substituted in equation (1) to obtain a first approximation of the stress σ_x, which in turn can be used in the creep law of the material to get a second approximation of the creep strain increment. Then again, the process can be repeated until convergence is reached. At the start of the next time step, the total inelastic strain will be equal to the initial plastic strain plus the accumulated creep strain during the previous time increments.

Creep Laws

Creep, the time dependent deformation and fracture of materials, is probably the most general type of material behavior. The current state of the art in inelastic high-temperature analysis requires that plasticity and creep constitutive equations be formulated largely on independent bases. However, elevated-temperature deformation is, essentially, the result of time-dependent processes where both plastic and creep behaviors are present simultaneously. Prior creep deformations influence subsequent plastic behavior and *vice versa* (Refs. 18, 19). Since only limited information is available on these mutual interactions, the two behaviors were modeled separately in this study, as already noted in the previous section.

Very little information is available in the literature on the creep behavior of high-strength, quenched and tempered steels such as HY-80 and HY-130. Only some data on the minimum creep rupture time are reported (Ref. 20). For stainless steels, on the other hand, numerous studies have been performed to investigate their elevated-temperature inelastic behavior. Uniaxial creep behavior of stainless steels during the primary and secondary stage can be modeled by an equation of the form:

$$\epsilon_x^c(\sigma_x,t,\theta) = f(\sigma_x,\theta)\,[1-e^{-r(\sigma_x,\theta)t}] + g(\sigma_x,\theta) \cdot t \quad (3)$$

where ϵ_x^c is the uniaxial creep strain, σ_x the applied stress, θ the test temperature and t the time. The functions $f(\sigma_x,\theta)$, $r(\sigma_x,\theta)$ and $g(\sigma_x,\theta)$ can be deduced from creep test data by curve fitting. Clinard *et al.* (Ref. 21), report the following representation at θ = 1100°F (594°C) for Type 304 stainless steels:

$$f(\sigma_x) = 5.436 \times 10^{-5}\sigma_x^{1.843}$$
$$r(\sigma_x) = 5.929 \times 10^{-5} \exp(0.2029\sigma_x) \quad (4)$$
$$g(\sigma_x) = 6.73 \times 10^{-9} [\sinh(0.1479\sigma_x)]^{3.0}$$

where σ_x is expressed in ksi (1 ksi = 6.894 MPa), t in hours and the creep strain (ϵ_x^c) in in./in. (mm/mm). Creep response to constant uniaxial compression is usually assumed to be identical to that in tension (actually a reflection of it with respect to the time axis).

For the complete description of the time dependent behavior of the material, a "hardening rule" is needed in order to predict the creep response when the stress levels are changing. The two most commonly used rules, time hardening and strain hardening, are strictly correct only in step changes of stress that are of long duration. Experimental evidence tends to support a strain hardening formulation for the case of Type 304 stainless steels. However, in our problem where small changes of stress take place at each infinitesimal time step, it was decided to adopt time-hardening for computational efficiency. Specifically, the creep strain increment $\Delta\epsilon_x^c(y)$ accumu-

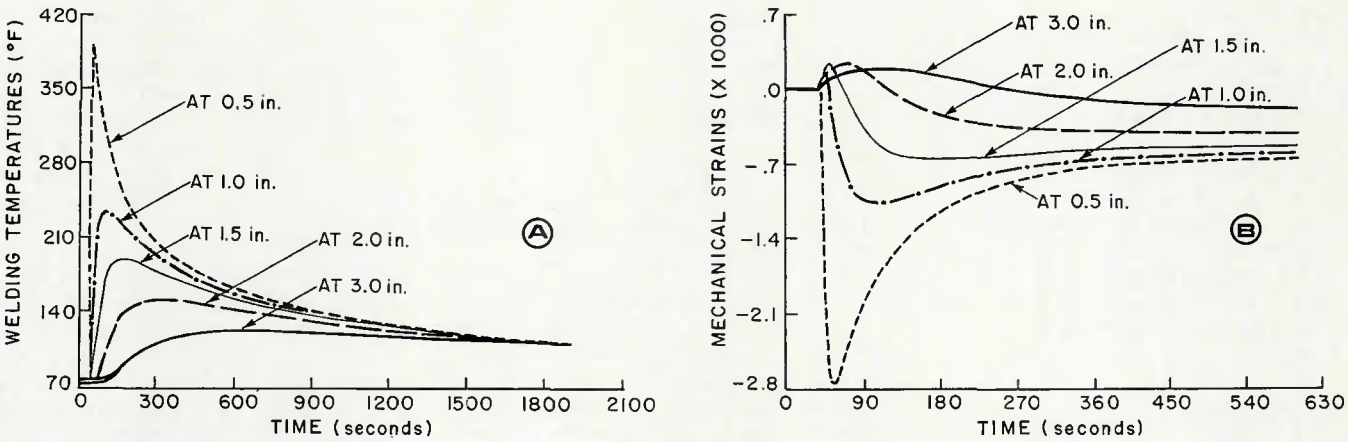

Fig. 4—Temperatures and mechanical strains as predicted by the one-dimensional program during edge welding of Type 304 stainless steel: A—temperatures; B—mechanical strains

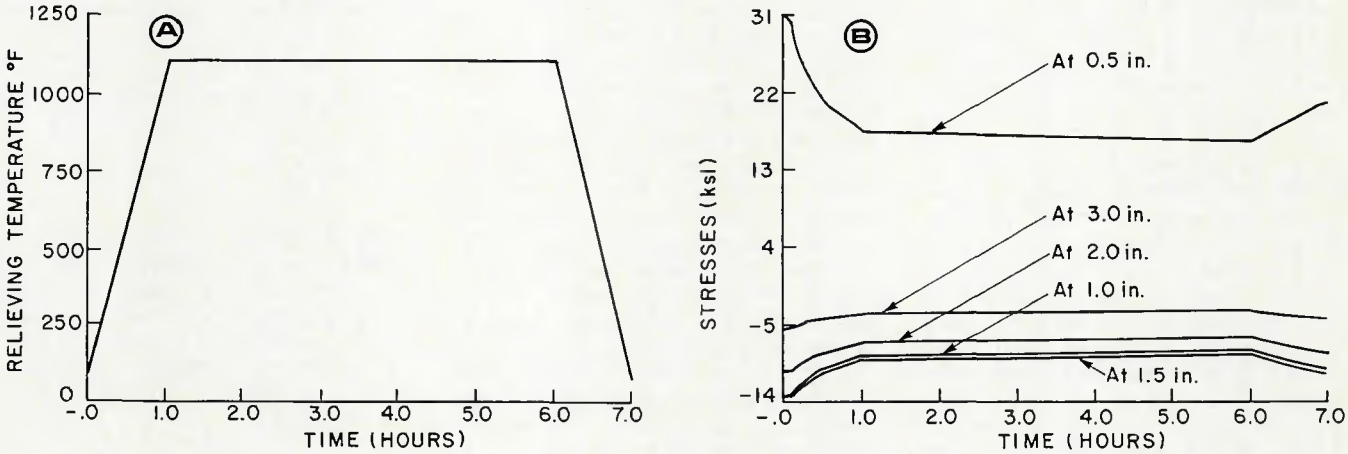

Fig. 5—Results of uniform heating at 1100°F (593°C) (Type 304 stainless steel): A—assumed temperatures; B—stresses as predicted by the one-dimensional program

lated between time t and t + Δt (at each point along the cross section) is:

$$\Delta\epsilon_x^c(y) = \epsilon_x^c[\sigma_x(y), t + \Delta t, \theta(y)] - \epsilon_x^c[\sigma_x(y), t, \theta(y)] \quad (5)$$

In the above equation, the creep strain rate $\Delta\epsilon_x^c(y)/\Delta t$ is a function of stress, time and temperature. Time hardening was assumed in order to avoid the added computations of solving equation (3) for time, as a strain hardening formulation would require.

Implementation and Results

In the computer implementation of the previously described model, most of the integrations were performed numerically. Significant simplifications were also possible in special cases due to symmetry or uniformity of the temperature distributions. Several sample cases were tested (Refs. 3, 4), and the results generally showed good correlation with experimental data for thin plates.

The predictions of the one-dimensional model for the case of edge welding and subsequent uniform temperature stress relief heat treatment of Type 304 stainless steel plates are presented here. Welding and stress relief heat treatment conditions were assumed exactly the same as in the stainless steel experiments described in the next section. Temperatures, strains, and stresses were calculated across a center strip of the specimen throughout welding and stress relief operations.

The assumed variation of material properties with temperature was obtained from the literature (Refs. 3, 21, 22, 23). A range of values was found for the arc efficiency and the surface heat loss coefficients. Since no experimental measurements of these parameters were made in this study, the actual selected values within that range were such as to minimize the deviation of the predicted welding temperature history from the experimentally measured one (Refs. 3, 4).

The predicted temperatures and mechanical strains during welding are plotted in Fig. 4. For ease of comparison with experimental data, the same locations of 0.5, 1.0, 1.5, 2.0 and 3.0 in. (12.7, 25.4, 38.1, 50.8 and 76.2 mm) from the weld line are selected. During the uniform stress relieving, the assumed temperature history is shown in Fig. 5A and the predicted variations in stress are plotted, versus time, in Fig. 5B. Comparisons of the predicted residual stress distribution after welding and after stress relieving are given in Fig. 6.

Experimental Study

Initial Verification Tests on Type 304 Stainless Steel Plates

To compare with the analytical predictions, initial experiments were performed using Type 304 stainless steel plates. The geometry and the dimensions of the main specimens are shown in Fig. 7. All plates were edge welded, and all but one were subsequently stress relieved in a furnace at different holding temperatures. The plates were finally sectioned, and residual stresses were measured by stress relax-

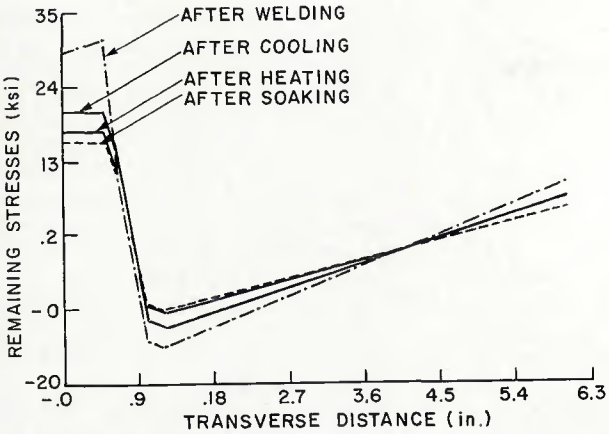

Fig. 6 — Comparison of residual stresses before, during, and after heating at 500°F (260°C) and at 1100°F (593°C) as predicted by the one-dimensional program (Type 304 stainless steel)

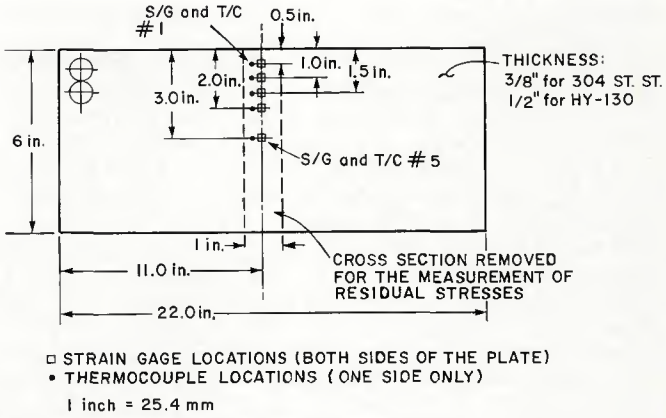

Fig. 7 — Specimen geometry and instrumentation

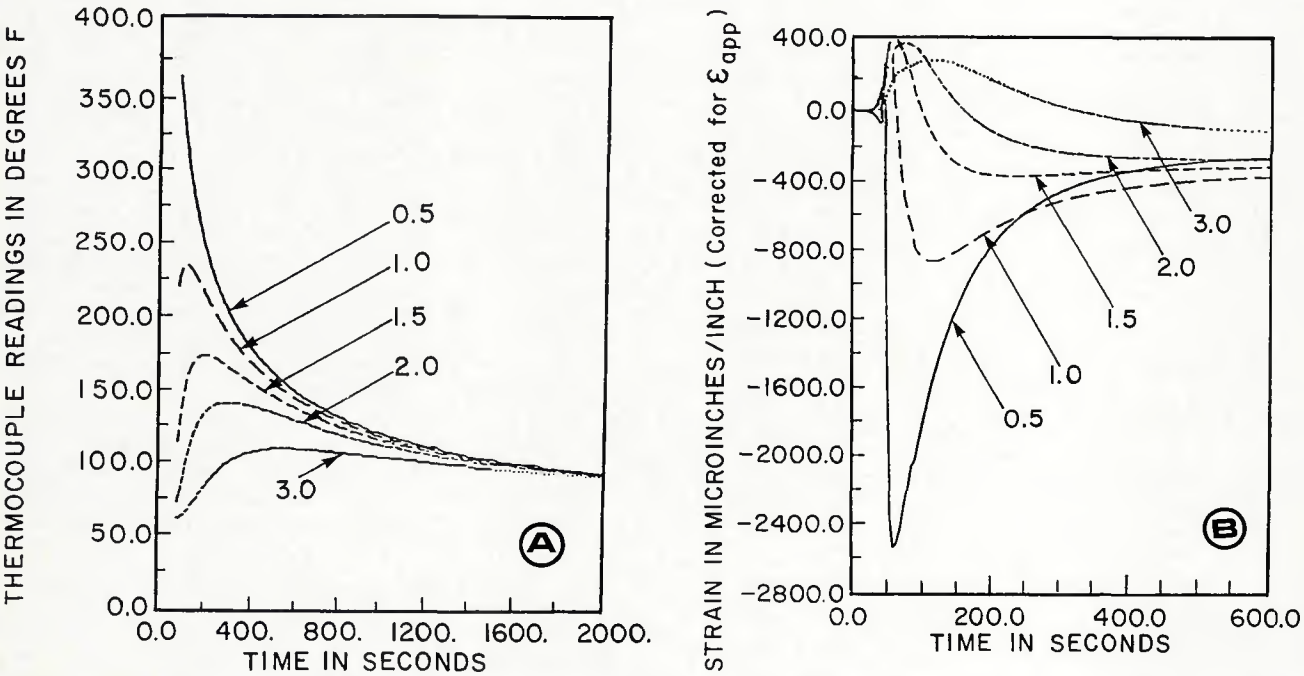

Fig. 8 — Results obtained during welding of specimen #2 (Type 304 stainless steel): A — measured temperatures; B — measured strains (strains corrected for temperature induced apparent strain and gage factor variations)

ation. The temperature and strain changes during welding and subsequent heat treatment were measured by thermocouples and electrical-resistance strain gages attached on the plates — Fig. 7. Failure of the strain gages at the high temperatures encountered near the weld line dictated positioning them at some distance away. This, however, prevented measurement of the tensile residual stress peaks.

Short-circuiting gas metal arc welding was performed on all specimens utilizing a 0.035 in. (0.89 mm) diameter Type 308 stainless steel welding wire, and a 90% He-7½% A-2½% CO_2 gas mixture. The finally selected welding conditions were the same for all specimens: arc voltage — 23 V, arc current — 90 A, welding wire feed speed — 175 ipm (4445 mm/s), and welding travel speed — 16 ipm (406.4 mm/s).

The observed temperature and strain histories, shown in Figure 8, for specimen #2, were almost identical in all specimens (Ref. 3). Based on this similarity in the

Table 1—Stress Relief Heat Treatment Conditions for the Verification Tests

Specimen number	Holding temperature °F (°C)	Time in Furnace, h
1	500°F (260°C)	6
2	Not stress relieved	—
3	Approx. 379°F (188°C)	4
4	1100°F (593°C)	7
6	500°F (260°C)	2
	370°F (188°C)	1

distribution of transient temperatures and strains, it is reasonable to assume that very similar residual stress distributions existed in all the specimens after welding.

After welding and cooling, one specimen (#2) was directly cut in order to determine the residual stresses in the as-welded condition, whereas the rest (specimens #1, #3 and #4) were stress relieved at different holding temperatures before cutting.

Details on the stress relief heat treatment conditions are given in Table 1. The temperature history during stress relieving is depicted in Fig. 9 for specimens #1, #3 and #4. Strain measurements during stress relieving were only taken for specimens #1 and #3, since the gages were destroyed at temperatures above 550°F (288°C). Strains for specimen #3, in particular, are shown in Fig. 10. Finally, after stress relieving, the destroyed gages were replaced, the plates were sectioned, and the obtained distribution of residual stresses was compared with the one in the as-welded case—Fig. 11.

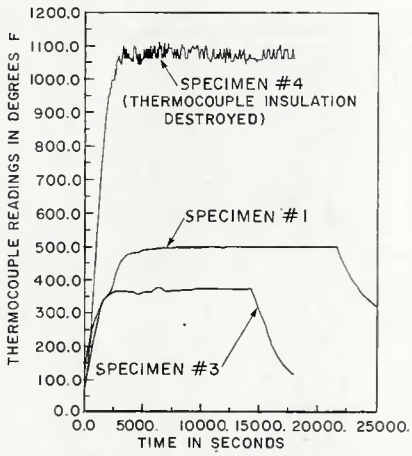

Fig. 9—Measured temperatures during heating of specimens #1, #3, and #4 (Type 304 stainless steel)

It should be noted at this point that austenitic stainless steels have to be heated to about 1650°F (900°C) to attain significant stress relief because of their good creep resistance. Only partial stress relief can be attained at temperatures lower than 1600°F (870°C). Best stress-relieving results are usually achieved by slow cooling. Nevertheless, an optimal stress relieving temperature is usually difficult to select, since the heat treatments that would provide adequate stress relief can be detrimental in terms of corrosion resistance; also, the ones that are not harmful to corrosion resistance may not provide adequate stress relief.

In the final selection of a proper stress relief heat treatment, due consideration must, therefore, be given not only to the material, itself, but also to the fabrication parameters and to the operating environment (Ref. 22). For Type 304 stainless steel in particular, stress relieving temperatures between 900°F (482°C) and 1000°F (538°C) are usually recommended in order to knock off the peak stresses and to ensure dimensional stability.

Further Experiments on HY-130 High Strength Steel Plates

The very high residual stresses that develop during welding of HY-130 quenched and tempered steels make stress relief heat treatments very attractive. Substantial reduction of stresses was shown to occur in both the base and weld metal at temperatures between 950°F (510°C) and 1050°F (566°C). However, a severe degradation of notch toughness may also occur at these temperatures. This embrittlement, which is phenomenologically similar to temper embrittlement, is believed to be influenced by the soaking temperature, the time at temperature, the cooling rates, the plastic strain, the exact alloy composition, and prior heat treatment.

Extensive investigation on the subject was performed by the U.S. Steel Corporation and the U.S. Navy (N.S.R.D.C. Materials Laboratory). Results by Rosenstein (Ref. 24) indicated that stress relief cycles are cumulative in nature; this conclusion was reached when comparing the tensile and Charpy properties resulting from consequent heat treatments of short duration and one single treatment of long duration, both having the same soaking times. Furthermore, it was observed that the degradation of notch toughness was maximum when stress relieving at 950°F (510°C) and minimum when at 1050°F (566°C). However, investigations of the effects of stress relieving on the weld metal have shown that the higher temperatures may substantially reduce the yield and tensile strength of the weld metal, and thus may cause undermatching. Therefore, the most practical temperature range for effective stress relieving of HY-130 weldments is between 1000°F (538°C) and 1025°F (552°C).

The geometry and the configuration of the tested HY-130 steel specimens is shown in Fig. 7. All plates were edge welded, and all but one were subsequently stress relieved by either uniform

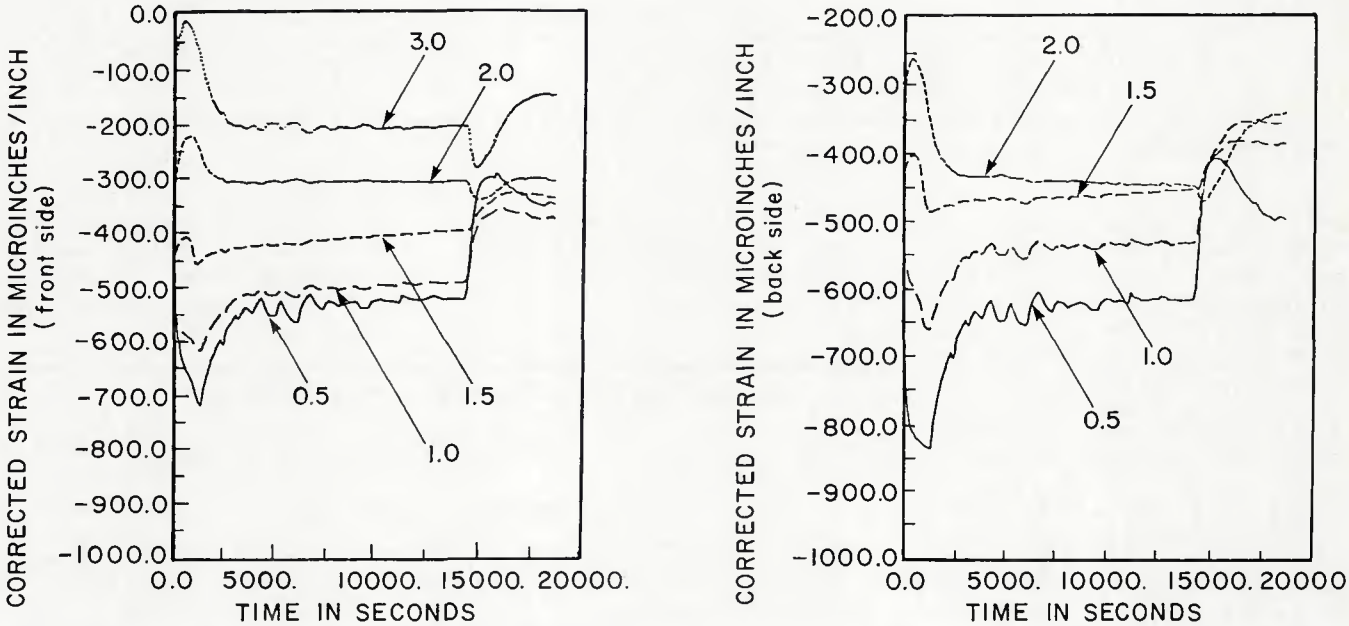

Fig. 10—Measured mechanical strain during heating of specimen #3 (Type 304 stainless steel). Strains were corrected for temperature induced strain and gage factor variations

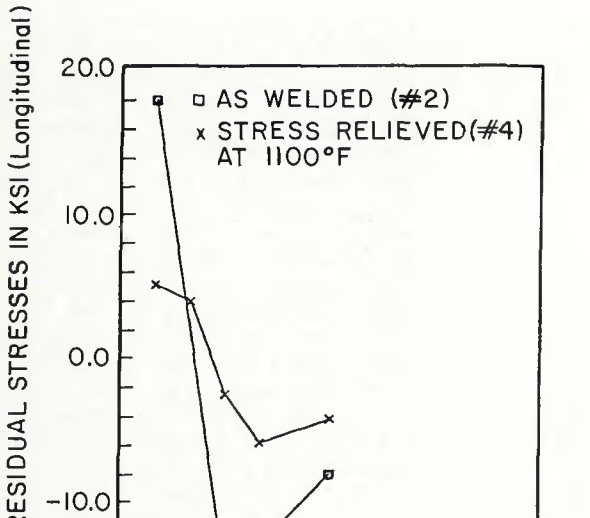

Fig. 11 — Comparison of measured longitudinal residual stresses after welding and after stress relief heat treatment (Type 304 stainless steel)

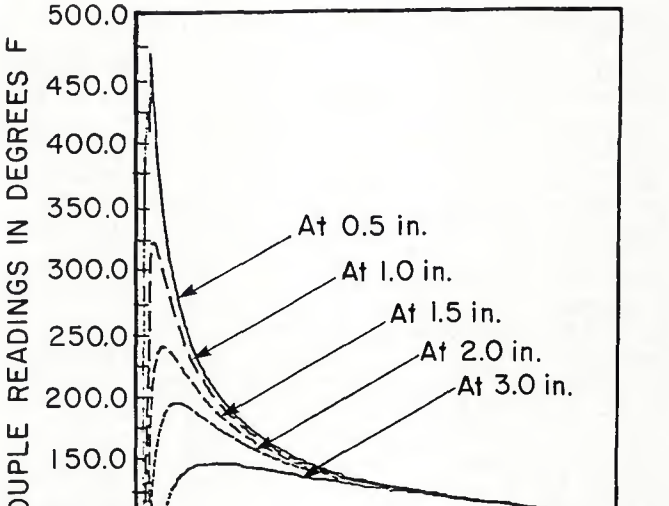

Fig. 12 — Measured temperatures during welding of specimen #2 (HY-130 steel)

heating or line heating by an oxyacetylene flame. The plates were then cut, and residual stresses were measured by stress relaxation. Only temperatures were measured during welding and stress relieving operations. Strain gages were installed on all specimens (in both the longitudinal and the transverse direction) only before cutting. Their location is again depicted in Fig. 7.

Spray-transfer gas metal arc welding was performed on all specimens utilizing 0.045 in. (1.145 mm) diameter Airco AX-140 welding wire and a 98% A–2% O_2 gas mixture. The selected welding conditions were (same for all specimens): arc voltage — 27 V, arc current — 225 A, welding wire feed speed — 285 ipm (120.7 mm/s), and welding travel speed — 21 ipm (8.9 mm/s).

The observed temperature distribution was very similar in all plates — Fig. 12.

After welding, specimen #1 was directly cut in order to determine the as-

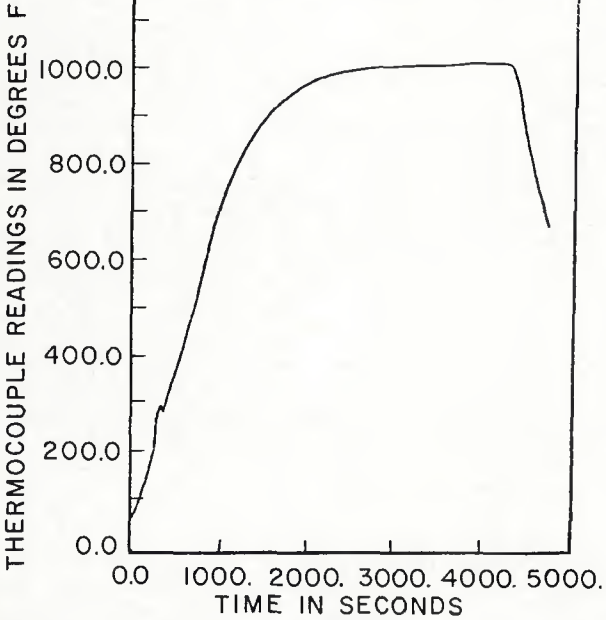

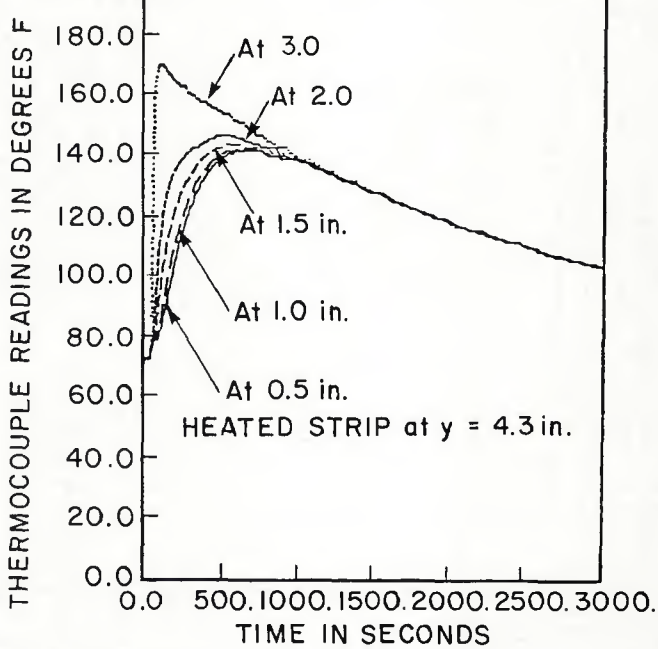

Fig. 13 — Measured temperatures during heating of specimen #2 (HY-130 steel): A — during uniform heating; B — during flame heating

welded residual stress distribution. Specimen #2 was heated in a furnace at 1000°F (538°C) and air cooled to room temperature. Since no comprehensive creep data were available for HY-130 steels, stress relaxation during uniform heating could not be handled by the analytical model. Thus, the plates were only left in the furnace until a uniform temperature of 1000°F (538°C) was attained.

Specimens #3 and #4, on the other hand, were flame heated using an oxy-acetylene torch. The torch was moved at a constant speed of 1 ipm (25.4 mm/min) along a line parallel to the weld center line and at a distance of 1.6 in. (40.6 mm) from it for specimen #3 and 4.3 in. (109.2 mm) for specimen #4. The selection of the torch velocity and location was based on analytical predictions for maximum stress relaxation (Ref. 4).

The temperature distributions during heating are shown in Fig. 13. The experimentally observed residual stress distributions are given, together with analytical predictions, in Figs. 14 and 15.

Computer-Aided Welding Experimentation

An important by-product of the experimental part of this study was the development of a highly flexible microcomputer-based data acquisition and processing system for welding and heat-treating experiments. In the past, light-writing oscillographs have almost exclusively been used as data recording devices during welding experiments. However, the simplicity of operation and the relatively low cost of these systems should be contrasted to the significant effort and time required for the manual data reduction. These considerations coupled with the availability of compact, powerful and inexpensive microcomputers led in the decision to develop a computer-aided data acquisition system.

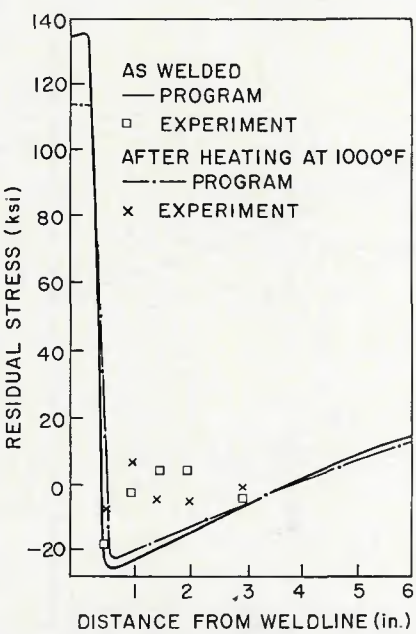

Fig. 14 — Longitudinal residual stresses after welding and after uniform heating at 1000°F (538°C) — (HY-130 steel)

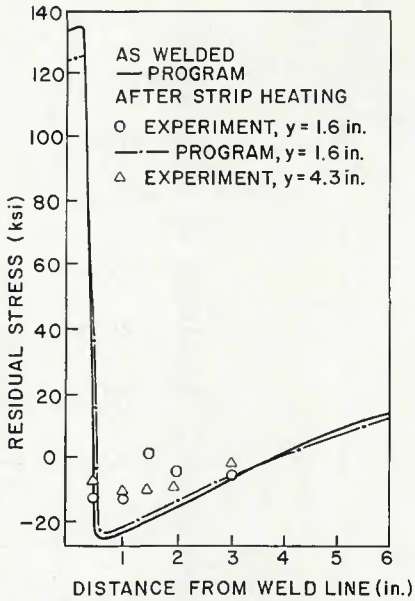

Fig. 15 — Longitudinal residual stresses after welding and strip heating (HY-130 steel)

The system would not only be used for recording temperatures, strains, displacements and welding conditions during experiments but would also ultimately become the necessary data acquisition and processing element in real-time welding process control applications. The main components of the configured modular system are:

1. A MINC-23 microcomputer manufactured by D.E.C.
2. A 9000 data acquisition system made by Daytronic Corporation.

Software and hardware were developed so that high speed data acquisition under various configurations was possible (Refs. 25, 26). Interfacing with other computers or test instruments, and use of the system for welding process control are directly feasible.

Conclusion

The study presented in this paper was an initial step towards an integrated approach in the analysis and control of welding residual stresses. The one-dimensional stress analysis was extended to calculate residual stresses not only after welding of thin plates but also after subsequent stress relief heat treatments. Although only uniform heating and line heating with a flame were examined, any temperature history and distribution during the treatment can be also assumed.

The one dimensional model is simple and, unlike finite element models, is very cost-effective in its computer implementation. Therefore, it allows for a series of parametric analyses to be performed and the relative importance of various parameters to be easily investigated. Some fine-tuning of the model is also possible through a limited number of experiments. Such features are essential when determining an optimal stress relieving treatment, where a properly selected heating pattern would maximize stress relief.

The analytical model can be effectively used as long as the previously outlined assumptions are not severely violated, especially with respect to the two-dimensionality of the temperature distribution and the one-dimensionality of stresses. The high temperature inelastic behavior of the material must also be well established and modeled, as was the case for the Type 304 stainless steels.

For the case of HY-130 high strength steels, the creep behavior was not modeled, and further investigation is needed before definite conclusions are drawn. It should be noted, however, that the one-dimensional welding model was found in the past (Ref. 1) as not being able to accurately predict the welding residual stress distribution in high strength quenched and tempered steels, especially in the area near the weld line. The observed discrepancies can be attributed to departure from the assumptions of the analytical model and the fact that phase transformations during cooling are not taken into account.

Analytical models for the study of welding residual stresses do not have the wide applicability and the predictive capability of numerical ones. Nonetheless, it should be noted that they are significantly less expensive to implement and thus can be readily employed in parametric analyses or in order to obtain a first approximation of the stress distributions. Furthermore, it should be mentioned that simple analytical models are also becoming increasingly important in augmenting simple feedback in control applications where capability for real-time implementation or closed-form representation is essential. Further work along the same lines is now under way in current M.I.T. research programs where simplified analytical models will be used in the control of temperature distribution and history during and after welding and in the control of laser forming of steel plates.

Acknowledgment

This study was performed as a final part of a 4½ year contract with the Office of Naval Research (Contract no.

N00014-75-C-0469). The authors gratefully acknowledge the financial support provided by O.N.R. Special thanks are also due to Mr. Kevin P. Carpentier who performed the HY-130 experiments, to Dr. Vassilios J. Papazoglou for his help in the heat source modeling, and to Ms. Muriel J. Bernier for her efforts in drawing the figures.

References

1. Masubuchi, K. 1980. *Analysis of welded structures—residual stresses, distortion and their consequences.* Oxford, England/New York, USA: Pergamon Press.

2. Agapakis, J. E., Papazoglou, V. J., Imakita, A., and Masubuchi, K. 1982 (Nov.). *Study of residual stresses and distortion in structural weldments in high strength steels.* Final report under Contract No. N00014-75-0469 (M.I.T. OSP #82558) to the Office of Naval Research, M.I.T.

3. Agapakis, J. E. 1982 (May). *Welding of high strength and stainless steels: a study on weld metal strength and stress relieving.* S.M. thesis, M.I.T.

4. Carpentier, K. P. 1982 (May). *Thermal stress relief of HY-130 weldments.* S.M. thesis, M.I.T.

5. Burdekin, F. M. 1969. *Heat treatment of welded structures,* 2nd ed. Abington, England: The Welding Institute.

6. Tanaka, J. 1972. Decrease in residual stresses, change in mechanical properties and cracking due to stress relieving heat treatment of HT-80 steel. *Welding in the World* 10(1/2).

7. Ueda, H., and Fukuda, K. 1975. Analysis of welding stress relieving by annealing based on finite element method. *Trans. of Japan Weld. Res. Inst.* 4(1): 39-45.

8. Fujita, Y., Nomoto, T., and Aoyagi, A. 1973 (May). *A study on stress relaxation due to heat treatment.* Dept. of Naval Architecture, University of Tokyo, IIW doc. X-697-73.

9. Cameron, I. G., and Pemberton, C. S. 1977. A theoretical study of thermal stress relief in thin shells of revolution. *Intl. J. for Num. Meth. in Eng.* 11: 1423-1437.

10. Josefson, B. L. 1982 (August). Residual stresses and their redistribution during annealing of a girth-butt welded thin walled pipe. *J. of Pressure Vessel Technology* 104: 245-250.

11. Imakita, A., Papazoglou, V. J., and Masubuchi, K. 1982 (July). One-dimensional computer programs for analyzing heat flow, transient thermal strains, residual stresses, and distortion in weldments. Report to ONR from M.I.T. prepared under Contract no. N00014-75-C-0469 (M.I.T. OSP No. 82558).

12. Rosenthal, D. 1941. Mathematical theory of heat distribution during welding and cutting. *Welding Journal* 20(5):220-s to 234-s.

13. Rosenthal, D. 1946 (Nov.). The theory of moving sources of heat and its application to metal treatment. *Transactions, ASME:* 849-866.

14. Mendelson, A. 1968. *Plasticity: theory and application,* New York: MacMillan Publ. Co.

15. Mendelson, A., Hirschberg, M. H., and Manson, S. S. 1959 (Dec.). A general approach to the practical solution of creep problems. *Transactions, ASME, Journal of Basic Engineering:* 585-598.

16. Tall, L. 1964. Residual stresses in welded plates, a theoretical study. *Welding Journal* 43(1): 10-s to 23-s.

17. Masubuchi, K., Simmons, F. B., and Monroe, R. E. 1968 (July). *Analysis of thermal stresses and metal movement during welding,* RSIC-820. Alabama: Redstone Scientific Information Center, Redstone Arsenal.

18. Corum, J. M., *et al.* 1974 (Dec.). *Interim guidelines for detailed inelastic analysis of high-temperature reactor system components.* Report ORNL-5014. Tennessee: Oak Ridge National Laboratory.

19. Pugh, C. E., *et al.* 1972 (Sept.). *Currently recommended constitutive equations for inelastic design analysis of FFTF components.* Report ORNL TM-3602. Tennessee: Oak Ridge National Laboratory.

20. Domis, W. F. 1968 (July). *Creep and creep rupture properties of HY-80 and HY-130 (T) steels.* Report No. 39.012-006 (1), U.S. Steel Applied Research Laboratory.

21. Clinard, J. A., *et al.* 1977 (Sept.). Verification by comparison of independent computer program solutions. *Pressure vessels and piping computer program evaluation and qualification, energy technology conference, Houston, Texas, A.S.M.E.:* 27-49.

22. American Society for Metals, 1981. *Metals handbook, volumes 1 and 4,* 9th ed.

23. Peckner, D., and Bernstein, I. 1977. *Handbook of stainless steels,* New York: McGraw Hill.

24. Rosenstein, A. H. 1970 (March). Phenomenological investigations of stress relief embrittlement. *Welding Journal* 49(3): 122-s to 131-s.

25. Agapakis, J. 1983 (March). *Fundamentals of computer aided experimentation for welding.* MIT Department of Ocean Engineering report No. 83-16.

26. Agapakis, J., and Masubuchi, K. 1983 (May). A flexible microcomputer-based data acquisition and processing system for welding experiments. Paper presented in the 1983 spring meeting of the Society for Experimental Stress Analysis, Cleveland, Ohio.

Appendix

A. Temperature Distribution During Welding and Line Heating

The Rosenthal solution (Refs. 12, 13) for the quasi-stationary temperature distribution in an infinitely large plate heated by a line heat source is based on the assumptions that:

1. The physical properties of the conducting medium are constant.
2. Heat losses to the surrounding atmosphere are neglected.
3. Phase changes and their accompanying absorption or release of latent heat are not taken into account.

Under these assumptions, the closed form solution of the conduction differential equation is:

$$\theta-\theta_o = \frac{Q}{2\pi kH} \cdot e^{-\lambda v \xi} \cdot K_o(\lambda v r) \qquad \text{(A-1)}$$

where θ_o is the initial temperature, Q the total heat input, v the welding speed, H the plate thickness, t the time, k the thermal conductivity, $\frac{1}{2}\lambda$ the thermal diffusivity ($\frac{1}{2}\lambda = k/\rho c$), ρ the density, c the specific heat, and $K_o(x)$ the modified Bessel function of second kind and zero order. In the moving coordinate system:

$\xi = x - vt$ and
$r = (\xi^2 + y^2)^{1/2}$

Heat losses to the atmosphere can be then taken into account by replacing in the Bessel function the factor λv by:

$$\left[(\lambda v)^2 + \frac{h_1 + h_2}{kH}\right]^{1/2}$$

where h_1 and h_2 are the heat transfer coefficients at the top and bottom of the plate respectively.

Further, in order to take into account the temperature dependence of material properties, an iterative approach is followed. Specifically, as detailed by Imakita *et al.* (Ref. 11), the fundamental heat source solution with material properties at some temperature—say 300°C (572°F)—provides the first approximate solution at a particular point. This temperature is compared with the initial guess and if the two temperatures differ by more than 0.5°C (0.9°F), new properties are found for a temperature halfway in between. These new values are used to obtain a new temperature estimate. The process is repeated until convergence is reached.

For the case of line heating, the temperature distribution can be calculated by modifying the Rosenthal solution for a point-heat source moving on a semi-infinite body:

$$\theta-\theta_o = \frac{Q}{2\pi k} \cdot e^{-\lambda v \xi} \cdot \frac{e^{-\lambda v R}}{R} \qquad \text{(A-2)}$$

where $R = (\xi^2 + y^2 + z^2)^{1/2}$ and all the other variables are the same as in equation (A-1).

To satisfy the adiabatic boundary conditions on the top, bottom, and sides of a finite plate, an infinite series of heat source images have to be added—Fig 3. The solution then becomes:

$$\theta = \theta_o + \frac{Q}{2\pi k} e^{-\lambda v \xi} \left[\frac{e^{-\lambda v R}}{R} + \sum_{n=1}^{\infty} \left[\frac{e^{-\lambda v R^T_n}}{R^T_n} + \frac{e^{-\lambda n R^B_n}}{R^B_n} \right] + \sum_{m=1}^{\infty} \left[\frac{e^{-\lambda v R^L_m}}{R^L_m} + \frac{e^{-\lambda v R^R_m}}{R^R_m} \right] + \sum_{n=1}^{\infty} \sum_{m=1}^{\infty} \left[\frac{e^{-\lambda v R^{TL}_{nm}}}{R^{TL}_{nm}} + \frac{e^{-\lambda v R^{TL}_{nm}}}{R^{TR}_{nm}} + \frac{e^{-\lambda v R^{BL}_{nm}}}{R^{BL}_{nm}} + \frac{e^{-\lambda v R^{BR}_{nm}}}{R^{BR}_{nm}} \right] \right] \quad \text{(A-3)}$$

where.

$$R^T_n = \sqrt{\xi^2 + y^2 + (2nH - z)^2}, \quad R^L_m = \sqrt{\xi^2 + (O^L_m - y)^2 + z^2}$$
$$R^B_n = \sqrt{\xi^2 + y^2 + (2nH + z)^2}, \quad R^R_m = \sqrt{\xi^2 + (O^R_m + y)^2 + z^2} \quad \text{(A-4)}$$
$$O^L_m = O^R_{m-1} + 2G \text{ with } O^L_1 = 2G, \quad O^R_m = O^L_{m-1} + 2F \text{ with } O^R_1 = 2F$$
$$R^{TL}_{nm} = \sqrt{\xi^2 + (O^L_m - y)^2 + (2nH + z)^2}, \quad R^{BL}_{nm} = \sqrt{\xi^2 + (O^L_m - y)^2 + (2nH + z)^2}$$
$$R^{TR}_{nm} = \sqrt{\xi^2 + (O^R_m + y)^2 + (2nH - z)^2}, \quad R^{BR}_{nm} = \sqrt{\xi^2 + (O^R_m + y)^2 + (2nH - z)^2}$$

B. One-Dimensional Stress Analysis

A one-dimensional stress distribution ($\sigma_x = \sigma_x(y)$) is assumed for an infinitely long plate subject to a temperature distribution $\theta(y)$ non-varying along its entire length. Compatibility equations for one-dimension reduce to:

$$\epsilon_x = c_1 + c_2 y \quad \text{(B-1)}$$

which essentially states that plane sections remain plane.

As was mentioned earlier, the following will hold along the cross section at the end of any time interval:

$$\sigma_x(y) = \quad \text{(B-2)}$$
$$E[\epsilon_x(y) - \alpha(\theta(y) - \theta_o) - \epsilon^{in}_x(y) - \Delta\epsilon^{in}_x(y)]$$

where all the variables have been previously defined.

It should be also noted that the inelastic strain is assumed to be composed of plastic and creep components:

$$\epsilon^{in}_x(y) = \epsilon^{pl}_x(y) + \epsilon^{c}_x(y) \quad \text{(B-3)}$$

From the global equilibrium on a cross section, it follows that:

$$\int_{-c}^{+c} \sigma_x \, dy = O$$
$$\int_{-c}^{+c} \sigma_x y \, dy = O \quad \text{(B-4)}$$

which together with (B-1) and (B-2) can give expressions for the determination of coefficients c_1 and c_2. In this way an expression for the total strain can be obtained, as in equation (2) of the paper, where:

$$A_1 = \int_{-c}^{+c} Ey^2 dy / B, \; A_2 = \int_{-c}^{+c} Eydy / B, \; A_3 = \int_{-c}^{+c} Edy / B$$

and:

$$B = \left[\int_{-c}^{+c} Edy \right] \cdot \left[\int_{-c}^{+c} Ey^2 dy \right] - \left[\int_{-c}^{+c} Eydy \right]^2$$

WRC Bulletin 284
April, 1983

The External Pressure Collapse Tests of Tubes

by E. Tschoepe and J. R. Maison

An experimental program was performed to confirm or refute the applicability of Figure UG-31 in Section VIII, Division 1 of the ASME Boiler and Pressure Vessel Code to the design of tubes under external pressure. Commercially available tubes were subjected to external pressure until collapse occurred. The data generated indicates the current ASME design rules for tubes under external pressure are suitable for continued application.

Publication of this report was sponsored by the Subcommittee on Shells of the Pressure Vessel Research Committee of the Welding Research Council.

The price of WRC Bulletin 284 is $12.00 per copy, plus $5.00 for postage and handling. Orders should be sent with payment to the Welding Research Council, Room 1301, 345 East 47th St., New York, NY 10017.